CSIRO PUBLISHING

www.publish.csiro.au/journals/ajc

Aust. J. Chem. **2011**, *64*, 1203–1210

Aggregation-Induced Emission and Biological Application of Tetraphenylethene Luminogens

Yuning Hong,[A] *Jacky Wing Yip Lam,*[A] *Sijie Chen,*[A] *and Ben Zhong Tang*[A,B,C]

[A]Department of Chemistry, Nano Science and Technology Program, Bioengineering Graduate Program, The Hong Kong University of Science and Technology, Clear Water Bay, Kowloon, Hong Kong, China.

[B]Department of Polymer Science and Engineering, Institute of Biomedical Macromolecules, Zhejiang University, Hangzhou 310027, China.

[C]Corresponding author. Email: tangbenz@ust.hk

Tetraphenylethene derivatives [Ph(PhCH=CHPhR)C=C(PhCH=CHPhR)Ph, R=H, CN, NO_2, NPh_2] with green, yellow-green, and orange emission colours were designed and synthesized. These molecules are practically non-emissive in their dilute solutions but emit intensely as nanoaggregates in poor solvents, demonstrating a novel phenomenon of aggregation-induced emission. Their blended films with poly(methyl methacrylate) also display bright emissions. Restriction of intramolecular motion in the condensed phase may be responsible for such unusual behaviour. Multilayer electroluminescence devices with a configuration of indium tin oxide/*N*,*N*′-di(1-naphthyl)-*N*,*N*′-diphenylbenzidine/emitter/tris(8-hydroxyquinolinolato)aluminum (Alq_3)/LiF/Al were constructed, which gave green light with a maximum luminance and current efficiency of 12930 cd cm^{-2} and 3.04 cd A^{-1} respectively. The tetraphenylethenes can serve as excellent cell staining agents for selectively illuminating the cytoplasm and vesicles of living cells.

Manuscript received: 29 April 2011.
Manuscript accepted: 21 May 2011.
Published online: 27 July 2011.

Introduction

The development of fluorescent materials is of critical importance to biological science and biotechnology because it offers a direct visualization tool for detecting biological macromolecules and monitoring biological events.[1] A large variety of materials, such as organic dyes, inorganic quantum dots (QD), fluorescent proteins (FP), and polymeric and silica nanoparticles have been studied as potential candidates for biosensory applications.[2]

Inorganic QD are highly emissive and photostable but inherently cytotoxic because they are typically composed of heavy metals and chalcogens (e.g. CdSe and PbS).[3] The capping agents used in the QD preparation, such as trioctylphosphine, can also be of biological concern. Similarly, the surfactants used in the fabrication of polymeric and silica nanoparticles, such as sodium dodecyl sulfate, are harmful to living cells, because they can stimulate cytolysis even at a concentration as low as 0.0005 %.[4] Recently, FP have attracted much attention because they can be genetically encoded to the target of interest. The use of FP, however, requires a complicated transfection process and their large size may interfere with the conformation and dynamics of the target.[5]

In contrast, organic dyes enjoy structural and property diversity and are easy to use.[6] Conventional organic luminophors often exhibit remarkably bright emission in dilute solutions but become weakly or even non-emissive when they are dispersed in aqueous media or aggregated in living cells.[7] The close proximity of the chromophores often induces non-radiative energy transfer, resulting in self-quenching of the luminescence.[8] This has limited the scope of their applications and it is therefore desirable to develop luminophores that can overcome this 'aggregation-caused emission quenching' problem.

Our group has worked on the development of efficient organic chromophores and has discovered an unusual phenomenon of aggregation-induced emission (AIE): a series of non-emissive linear and cyclic π-conjugated organic polyenes including siloles, butadienes, 4*H*-pyrans, fulvenes, and tetraphenylethenes (TPE) are induced to emit efficiently by aggregate formation.[9] Attracted by this fascinating phenomenon, many groups have worked on AIE materials and done a great deal of outstanding work.[10] Among these, the TPE system has drawn much of our interest because TPE are stable, easy to make and readily functionalized, and exhibit appreciably high quantum yields.[9g,11] Thanks to the research efforts of scientists, TPE has been functionalized with ionic or polar functional groups to endow it with good water solubility.[12,13] These fluorophores have been successfully used as fluorescent probes for nucleic acid detection, enzymatic activity assay, and metallic ion tracing.[12,13] Most of these TPE derivatives, however, emit blue light. To expand their applications as light-emitting materials and in cell imaging, varied emission colours are highly desirable. This may be achieved by extension of their electronic conjugation through attachment of different substituents. In this work, we report the synthesis of TPE with various substituents on the peripheral phenyl rings and present their optical properties (Scheme 1). These new molecules show AIE features and can be used for the construction of electroluminescence (EL)

10.1071/CH11170

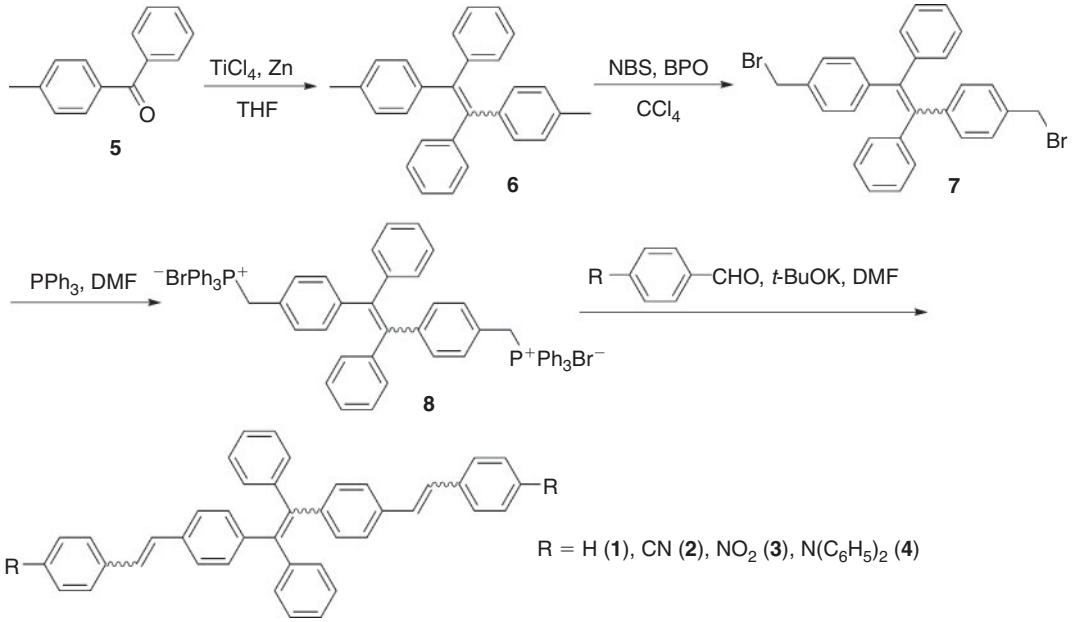

Scheme 1. Synthetic route to tetraphenylethene (TPE) derivatives **1**–**4**.

devices. Although they are not soluble in water, they work well as fluorescent stains for intracellular imaging and can selectively light up the cytoplasm and vesicles inside living HeLa cells without interference with their proliferation process.

Experimental

Materials and Instruments

THF (Labscan) was purified by simple distillation from sodium benzophenone ketyl under nitrogen immediately before use. Zinc dust, titanium(IV) chloride, *N*-bromosuccinimide (NBS), benzoyl peroxide (BPO), triphenylphosphine (PPh_3), benzaldehyde, 4-cyanobenzaldehyde, carbon tetrachloride, 4-nitrobenzaldehyde, triphenylamine, *N*,*N*-dimethylformamide (DMF), dichloromethane (DCM), dimethylsulfoxide (DMSO), and other reagents were all purchased from Aldrich and used as received.

^1H and ^{13}C NMR spectra were measured on a Bruker ARX 300 spectrometer in $CDCl_3$ using tetramethylsilane (TMS; $\delta = 0$ ppm) as the internal standard. Mass spectra were recorded on a Finnigan TSQ 7000 triple quadrupole spectrometer operating in fast-atom bombardment (FAB) mode. UV-vis spectra were measured on a Milton Roy Spectronic 3000 Array spectrophotometer. Photoluminescence (PL) spectra were recorded on a Perkin–Elmer LS 50B spectrofluorometer with a xenon discharge lamp excitation.

Synthesis

The TPE derivatives **3**–**6** were prepared according to Scheme 1. Typical procedures for their synthesis are shown below.

*1,2-Bis(4-methylphenyl)-1,2-diphenylethene **6***

A suspension of 4-methylbenzophenone (**5**, 3.6 g, 10.0 mmol), $TiCl_4$ (1.9 g, 10.0 mmol), and Zn dust (1.3 g, 20.0 mmol) in dry THF (100 mL) was refluxed for 20 h. Afterward, the reaction mixture was cooled to room temperature and filtered. The filtrate was evaporated and the crude product was purified on a silica-gel column using dichloromethane as eluent. Compound **6** was isolated as white solid in 94 % yield. δ_H (300 MHz, $CDCl_3$) 7.11–7.00 (m, 10H), 6.91 (d, 8H), 2.26 (d, 6H). δ_C (75 MHz, $CDCl_3$) 144.8, 141.6, 141.1, 136.6, 132.0, 131.9, 129.0, 128.2, 126.9, 21.9. *m*/*z* (FAB) 360.2 [M^+]; calc. 360.2.

*1,2-Bis[4-(bromomethyl)phenyl]-1,2-diphenylethene **7***

To a mixture of **6** (1.8 g, 5.0 mmol) and NBS (1.7 g, 10.0 mmol) in CCl_4 was added catalytic amount of BPO at room temperature. The mixture was stirred and heated to reflux for 8 h. After filtration and solvent evaporation, the product was purified by silica gel chromatography using DCM/hexane (1:4 v/v) as eluent. Compound **7** was isolated as pale yellow solid in 43 % yield. δ_H (300 MHz, $CDCl_3$) 7.14–7.07 (m, 10H), 7.02–6.96 (m, 8H), 4.41 (d, 4H). δ_C (75 MHz, $CDCl_3$) 144.4, 143.9, 141.5, 136.6, 132.3, 132.0, 129.2, 128.5, 127.4, 34.3. *m*/*z* (FAB) 518.0 [M^+]; calc. 518.2.

*1,2-Bis[4-(2-phenylvinyl)phenyl]-1,2-diphenylethene **1***

Triphenylphosphonium salt **8** was prepared from **7** and triphenylphosphine in DMF at 100°C. After stirring for 24 h, the solution was poured into large amount of toluene. The white precipitate was collected and directly used for the next reaction without purification. Into another round-bottom flask were added benzaldehyde (0.1 g, 0.94 mmol), **8** (0.1 g, 0.19 mmol), and a catalytic amount of 18-crown-6 in DMF (8 mL) under nitrogen. The solution was cooled to 0–5°C with an ice bath, into which potassium *t*-butoxide (0.056 g, 0.50 mmol) was added. The mixture was stirred under nitrogen at room temperature for 48 h and poured into a large amount of water. The precipitate was collected and the crude product was purified on a silica gel column using hexane as eluent. Yellow solid of **1** was obtained in 78 % yield. δ_H (300 MHz, $CDCl_3$) 7.46 (d, 2H), 7.40 (s, 2H), 7.32 (t, 2H), 7.23 (m, 2H), 7.19–7.17 (m, 6H), 7.15–7.10 (m, 6H), 7.06–6.97 (m, 8H), 6.88–6.85 (m, 2H), 6.51–6.49 (m, 2H). δ_C (75 MHz, $CDCl_3$) 143.5, 142.6, 140.8, 137.3, 135.3, 131.5, 130.0, 129.5, 128.7, 128.1, 127.6, 127.3, 127.0, 126.5, 125.8. *m*/*z* (FAB) 536.3 [M^+]; calc. 536.7.

Compounds **2**–**4** were prepared by similar procedures to those described above using appropriate aldehydes.

1,2-bis{4-[2-(4-cyanophenyl)vinyl]phenyl}-1,2-diphenylethene ***2***: Yellow solid; yield 85 %. δ_H (300 MHz, $CDCl_3$) 7.98–7.82 (m, 4H), 7.67–7.62 (m, 2H), 7.54–7.51 (m, 2H), 7.47–7.44 (m, 2H), 7.17–7.14 (m, 6H), 7.08–7.02 (m, 6H), 6.95–6.91 (m, 4H), 6.65 (d, 2H), 6.48 (d, 2H). δ_C (75 MHz, $CDCl_3$) 144.7, 144.1, 142.6, 141.6, 135.1, 133.6, 133.2, 132.6, 132.0, 130.3, 128.8, 128.5, 127.4, 127.0, 119.7, 111.0. *m/z* (FAB) 587.2 $[M^+]$; calc. 586.7.

1,2-Bis{4-[2-(4-nitrophenyl)vinyl]phenyl}-1,2-diphenylethene ***3***: Orange solid; yield 66 %. δ_H (300 MHz, $CDCl_3$) 8.19 (d, 4H), 8.04 (d, 4H), 7.58 (d, 4H), 7.31–7.26 (m, 4H), 7.19–7.14 (m, 4H), 7.08–7.03 (m, 4H), 6.95–6.91 (m, 2H), 6.70 (d, 2H), 6.53 (d, 2H). δ_C (75 MHz, $CDCl_3$) 146.7, 144.5, 144.1, 143.7, 143.5, 141.2, 134.5, 133.9, 133.2, 131.6, 129.8, 128.3, 127.0, 126.2, 124.0. *m/z* (FAB) 627.1 $[M + 1]^+$; calc. 627.1.

4-(Diphenylamino)benzaldehyde (reactant for the synthesis of **4**) was prepared by formylation of triphenylamine following the Vilsmeier–Haack procedure. White solid; yield 67 %. δ_H (300 MHz, $CDCl_3$) 9.81 (s, 1H), 7.68 (d, 2H), 7.37–7.32 (m, 4H), 7.19–7.15 (m, 6H), 7.01 (d, 2H). δ_C (75 MHz, $CDCl_3$) 191.2, 146.9, 132.0, 130.4, 129.8, 127.0, 125.8, 124.9, 120.0.

1,2-Bis{4-[2-(4-diphenylaminophenyl)vinyl]phenyl}-1,2-diphenylethene ***4***: Yellow solid; yield 50 %. δ_H (300 MHz, $CDCl_3$) 7.68 (d, 4H), 7.37–7.32 (m, 8H), 7.29–7.23 (m, 4H), 7.19–7.17 (m, 8H), 7.11–7.09 (m, 8H), 7.03–7.00 (m, 12H), 6.96–6.87 (m, 4H), 6.42 (m, 2H). δ_C (75 MHz, $CDCl_3$) 148.3, 148.0, 144.4, 143.6, 141.3, 136.3, 132.5, 132.0, 130.5, 130.0, 128.5, 128.4, 128.0, 127.5, 126.3, 125.3, 124.2, 123.7, 123.3. *m/z* (FAB) 872.0 $[M + 1^+]$; calc. 872.1.

Preparation of TPE-Doped Poly(methyl methacrylate) Films

The TPE-doped poly(methyl methacrylate) (PMMA) films were prepared by dissolving PMMA and TPE derivatives (10:1 by weight) in chloroform and then spin-coating the resultant solutions onto quartz plates.

Device Fabrication

The devices were fabricated on 80-nm indium tin oxide (ITO)-coated glass with a sheet resistance of 25 $\Omega\,sq^{-1}$. Prior to loading into the pretreatment chamber, the ITO-coated glass was soaked in detergent and ultrasonicated for 30 min, followed by spraying with de-ionized water for 10 min, soaking in water and ultrasonicated de-ionized water for 30 min, and oven-baking for 1 h. The cleaned samples were treated with perfluoromethane (CF_4) plasma with a power of 100 W, gas flow of 50 sccm, and pressure of 0.2 Torr (26.6 Pa) for 10 s in the pretreatment chamber. The samples were transferred to the organic chamber with a base pressure of 7×10^{-7} Torr for the deposition of *N*,*N*-bis(1-naphthyl)-*N*,*N*-diphenylbenzidine (NPB), 2,9-dimethyl-4,7-diphenyl-1,10-phenanthroline (BCP) and tris(8-hydroxyquinolinolato)-aluminium (Alq_3), which serve as hole-transport, hole-block, and electron-transport layers respectively. The samples were then transferred to the metal chamber for cathode deposition, which was composed of lithium fluoride (LiF) capped with aluminium (Al). The light-emitting area was 4 mm^2. The current density–voltage characteristics of the devices were measured with a HP4145B semiconductor parameter analyzer. The forward-direction photons emitted from the devices were detected by a calibrated UDT PIN-25D silicon photodiode. The luminance and external quantum efficiencies of the devices were inferred from the photocurrent of the photodiode. The electroluminescence spectra were obtained with a PR650 spectrophotometer. All measurements were carried out under air at room temperature without device encapsulation.

Cell Imaging

HeLa cells were grown overnight on a plasma-treated 25-mm round coverslip mounted onto a 35-mm Petri dish with an observation window. The living cells were stained with either 5 μM of **2** or **4** (by adding 2 μL of a 5 mM stock solution of **2** or **4** in DMSO to 2 mL culture) for 30 min to 5 h. The cells were imaged under an upright fluorescence microscope (Olympus BX41) or an inverted fluorescence microscope (Nikon Eclipse TE2000-U) using the combination of excitation and emission filters: excitation wavelength = 330–380 nm, diachronic mirror = 400 nm. The images of the cells were captured using a computer-controlled SPOT charged-couple device camera (Spot RT SE 18 Mono).

Results and Discussion

Dye Synthesis

We synthesized four TPE derivatives with different substituents on the peripheral phenyl rings and designed a multistep reaction route for their synthesis. TPE derivatives **1**–**4** were prepared according to the synthetic route shown in Scheme 1. 1,2-Bis(4-methylphenyl)-1,2-diphenyl-ethene (**6**) was first synthesized from McMurry coupling of 4-methylbenzophenone (**5**) using titanium(IV) chloride and zinc dust as catalysts. Bromination of **6** gave **7**, whose reaction with triphenylphosphine in DMF generated triphenylphosphonium salt **8**. Wittig reactions of **8** with the corresponding benzaldehydes in the presence of potassium *tert*-butoxide furnished TPEs **1**–**4** in 50–85 % yields. All the reactions proceeded smoothly and the desired products were isolated in satisfactory to high yields. We characterized the products by NMR and mass spectroscopy and all of them gave satisfactory analysis data corresponding to their molecular structures. The lipophilic TPE derivatives are completely soluble in common organic solvents such as acetonitrile, chloroform, and THF, slightly soluble in methanol and ethanol, but insoluble in water.

Aggregation-induced Emission

All the TPE are practically non-emissive when molecularly dissolved in good solvents but emit intensely in the aggregate state. An example of the UV and PL spectra of **1** is given in Fig. 1.

The acetonitrile solution of **1** emits dimly at ~415 nm when photoexcited at 370 nm. When 99 % water is added to the acetonitrile solution, an intense PL signal is recorded at 511 nm under the same measurement conditions. As **1** is insoluble in water, aggregates must have been formed in aqueous mixtures with high water contents. The solution is, however, homogeneous with no precipitates, suggesting that the aggregates are of nanodimension. The formation of nanoaggregates can be inferred from the level-off tail observed at the longer wavelength in the UV spectrum in an acetonitrile/water mixture with a 99 % water fraction. To have a quantitative picture, we measured its fluorescence quantum yield (Φ_F). The Φ_F in acetonitrile solution is as low as 0.48 %, revealing that **1** is a genuinely weak emitter in the solution state. The Φ_F remains unchanged when up to 50 % water is added (Fig. 2). Afterward, the value increases swiftly. At 90 % water fraction, the Φ_F value rises to ~26 %. The AIE effect can be quantified

by the extent of emission enhancement (α_{AIE}),[14] as defined below:

$$\alpha_{AIE} = \frac{\Phi_{F,a}}{\Phi_{F,s}}, \quad (1)$$

where $\Phi_{F,a}$ and $\Phi_{F,s}$ are the quantum yields in the aggregate and solution states respectively. From Eqn 1, the α_{AIE} value for **1** was calculated to be 53.8.

Careful observation reveals that the Φ_F value decreases slightly when the water content is raised to ~99 %, probably owing to the change in the packing order of the aggregates from a crystalline state to an amorphous one.[15] At a 'lower' water ratio, the molecules may have sufficient time to assemble in an ordered fashion to form more emissive crystalline clusters, whereas at a 'higher' water ratio, the molecules may abruptly agglomerate in a random way to form less emissive amorphous powders.

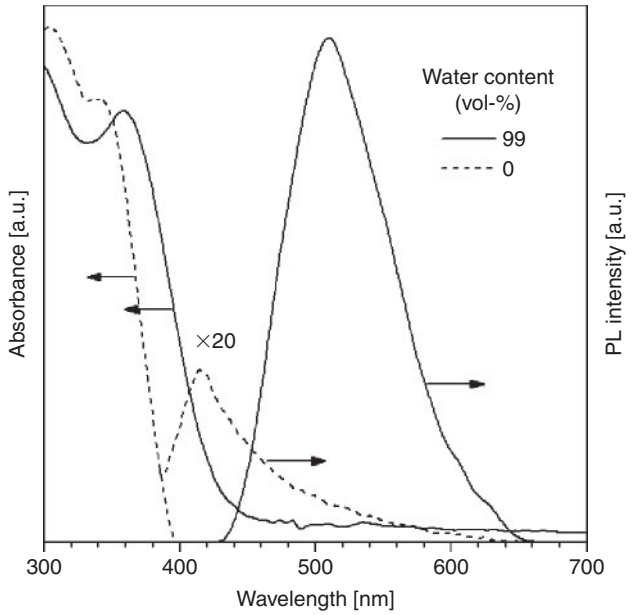

Fig. 1. UV and photoluminescence (PL) spectra of 1 in pure acetonitrile (dashed line) and acetonitrile/water mixture (1:99 v/v; solid line); concentration, 1:2.5 μM; excitation wavelength, 370 nm. Arrows pointing left indicate the curves are UV spectra. Arrows pointing right indicate the curves are PL spectra. The PL spectrum of 1 in pure acetonitrile is magnified by 20-fold.

Similar phenomena are observed in **2**–**4** (Table 1) and all of these are AIE-active. The maximum wavelength of emission of **2** in 99 % aqueous mixture is ~10 nm red-shifted from that of **1**, suggestive of its higher conjugation due to the electronic communication between the polarized cyano groups and the ethene core. The emission of **3** is observed at an even longer wavelength. Its Φ_F value in the aggregate state is, however, five-fold lower than **1**, which is in some sense understandable because nitro groups are known to induce intersystem crossing and cause non-radiative transition. Among the molecules, **4** shows the smallest α_{AIE} value because its dilute solution shows comparably stronger emission owing to the contribution from the triphenylamine unit. Although **4** emits more efficiently when aggregated in poor solvent, the associated Φ_F value is similar to those of **1** and **2**. These two effects thus mainly contribute to the lower α_{AIE} value of **4**. Fig. 2 shows the photographs of acetonitrile/water mixtures (1:99 v/v) of **1**–**3** taken under UV illumination. Whereas **1** and **2** emit cyan and green light, **3** is an orange emitter, demonstrating that the optical properties of TPE can be readily tuned by molecular engineering alteration of its structure.

To gain insight into the mechanism of the AIE effect, we doped TPE derivatives **1**–**4** into PMMA film (10 % by weight), in which PMMA serves as a solid 'solvent' to disperse the TPE molecules and impede their aggregate formation. Similarly to their nanoaggregates in the suspensions (Table 1), all the TPE-doped PMMA films emit bright light on photoexcitation, suggesting that intermolecular interactions play little role in their photophysical properties and the AIE phenomenon results from the restriction of intramolecular rotations, which blocks the non-radiative relaxation processes and hence boosts their PL efficiency.

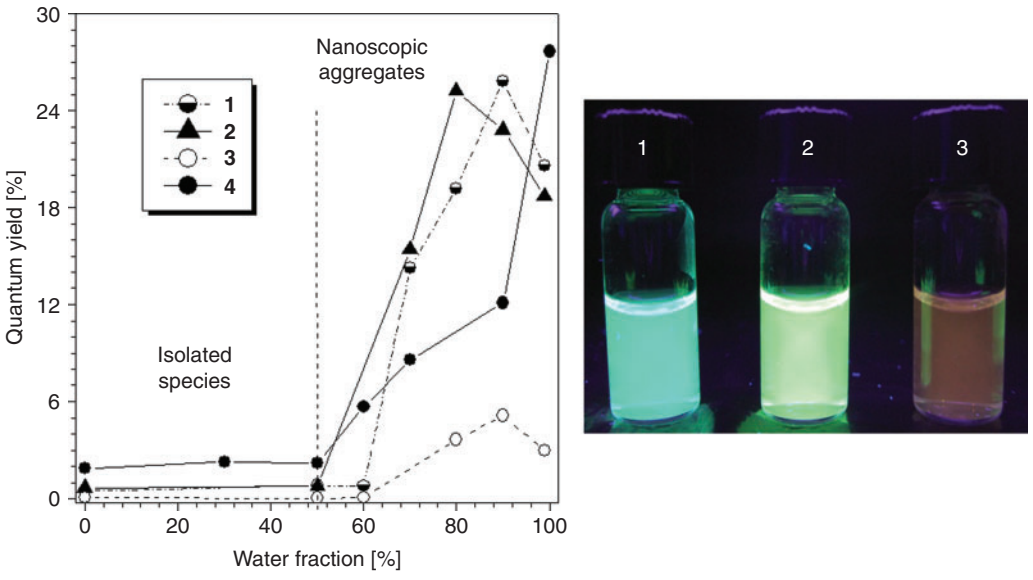

Fig. 2. Dependence of quantum yields of **1**–**4** on solvent compositions of acetonitrile/water mixtures. Photographs of **1**–**3** in acetonitrile/water mixture (1:99 v/v) taken under 365-nm UV illumination; dye concentration, 2.5 μM; excitation wavelength, 370 nm.

The AIE feature of the TPE derivatives prompted us to explore their application in light-emitting diodes. We studied their EL by fabrication of multilayer devices with a configuration of ITO/NPB (60 nm)/TPE (30 nm)/BCP (20 nm)/Alq_3 (20 nm)/LiF (1 nm)/Al (150 nm). As shown in Fig. 3, the EL spectrum of **2** peaks at ~520 nm. The device is turned on at ~10 V and radiates brilliantly with a luminance of up to 12930 cd cm^{-2} at ~18 V. The maximum current efficiency attained by the device is 3.04 cd A^{-1}, which is equivalent to a power efficiency of 0.87 lm W^{-1} at a current density of ~45 A m^{-2} and an applied voltage of ~11 V. Disappointingly, only weak EL was detected in the devices of other luminogens. The exact reason, however, is unknown at present.

Cell Imaging

The TPE derivatives are not soluble but form highly emissive nanoaggregates in aqueous medium, which inspired us to explore their application as fluorescent stains for living cell imaging. As **2** and **4** possess higher quantum efficiencies in the aggregate state, we chose them for the study. The nanoaggregates of **2** and **4** were prepared in Minimum Essential Medium (Sigma–Aldrich)/DMSO mixtures and the HeLa cells were imaged using a standard cell-staining protocol. The living cells were incubated with **2** or **4** (5 μM) for 5 h and then washed three times with phosphate buffered saline solution. As shown in Fig. 4a and c, the living cells grow normally even in the presence **2** or **4**, indicating that the TPE pose no toxicity to living cells.

The fluorescent images were taken on an upright fluorescence microscope under UV illumination. Although both **2** and **4** are yellowish-green emitters in the aggregate state (cf. Fig. 2), after entering the cell membrane, their emission colour changes to blue (Fig. 4b and d). The change in the emission colour can be discerned from Fig. 4d, where the extracellular nanoaggregates exhibit strong yellow emission. This phenomenon is commonly observed in TPE-based stains. It is plausible that the macromolecular crowding environment in the interior of the cell forces the dye molecules to adopt a more twisted conformation, thus resulting in emission in the shorter-wavelength region.[16] The performance of **2** is much better than **4** in terms of emission intensity. Thus, we used **2** for further investigation.

Table 1. Optical properties of 1–4 in solution (Soln), aggregate (Aggr), and film states
$\Phi_{F,a}$ and $\Phi_{F,s}$, quantum yields in the aggregate and solution states respectively

	λ_{ab} [nm][D]			λ_{em} [nm][E]			Film
	Soln[A]	Aggr[B]	Film[C]	Soln ($\Phi_{F,s}$)	Aggr ($\Phi_{F,a}$)	$\Phi_{F,a}/\Phi_{F,s}$	
1	335	359	365	415 (0.48)	511 (25.8)	53.8	476
2	334	370	395	418 (0.66)	521 (25.3)	38.3	496
3	380	404	443	467 (0.07)	586 (5.13)	73.3	540
4	383	390	419	517 (1.85)	525 (27.7)	15.0	502

[A]In acetonitrile solutions (2.5 μM).
[B]In acetonitrile/water mixtures (1:99 v/v, 2.5 μM).
[C]Blended with PMMA (poly(methyl methacrylate); 10 % by weight).
[D]Absorption maximum.
[E]Emission maximum with quantum yield (Φ_F, %) given in parentheses. The Φ_F values were determined using quinine sulfate (for **1** and **2**), fluorescein (for **3**) and 9,10-diphenylanthracene (for **4**); excitation wavelength: 370 nm.

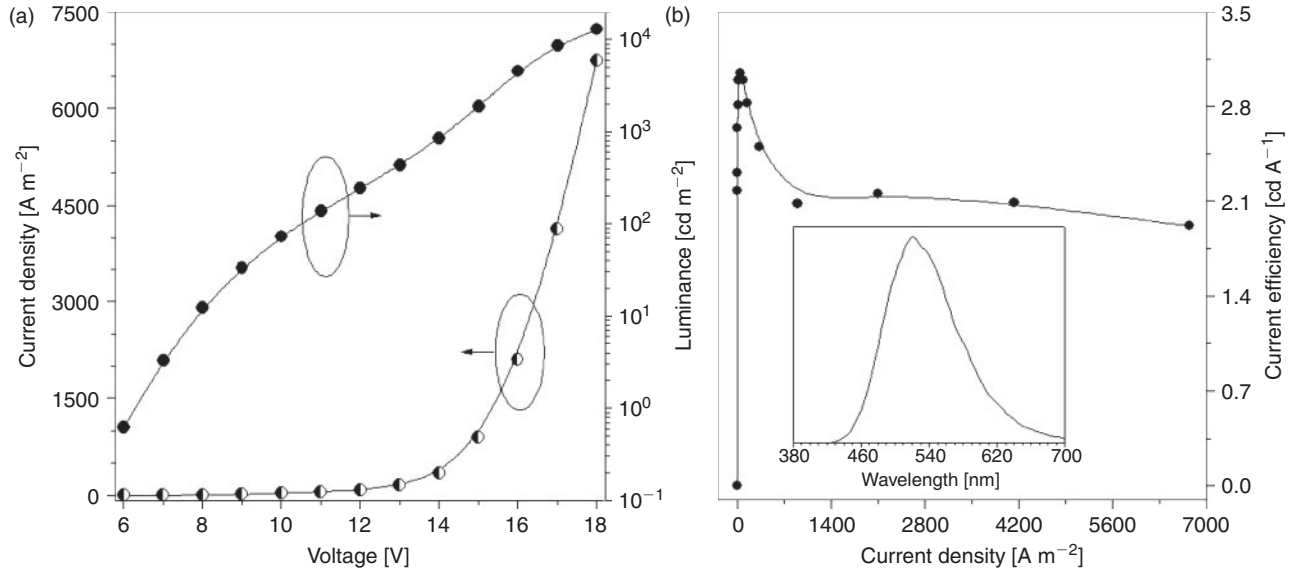

Fig. 3. (a) Change in current density and luminance with voltage, and (b) current efficiency versus current density curve of a multilayer electroluminescence (EL) device of 2. Inset in panel (b): EL spectrum of the device. Arrow pointing left indicates the curve is current density and arrow pointing right indicates the curve is luminance. The circles represent the whole curves.

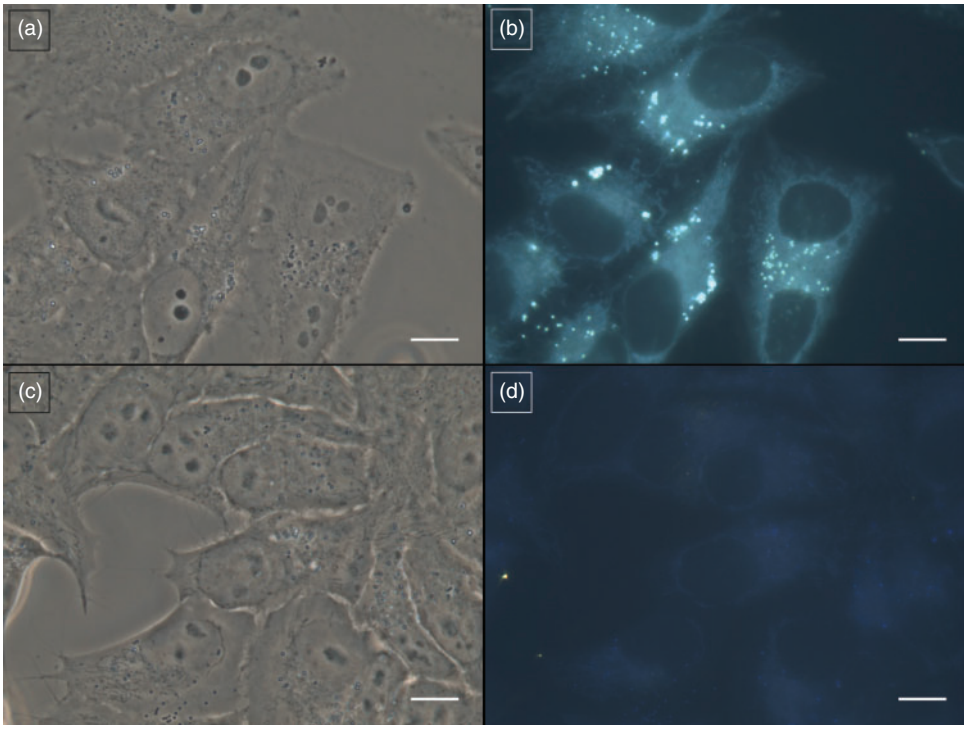

Fig. 4. (a and c) Phase contrast and (b and d) fluorescence images of HeLa cells stained with (a and b) **2** and (c and d) **4** for 5 h. Scale bar = 10 μm; [dye] = 5 μM.

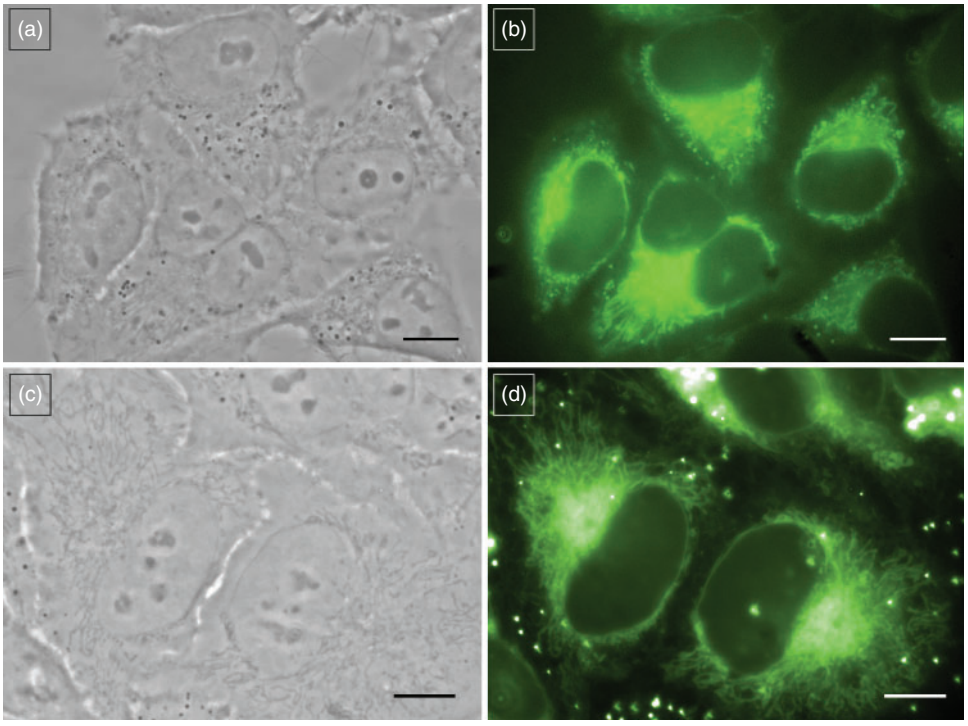

Fig. 5. (a and c) Phase contrast and (b and d) fluorescent images of HeLa cells stained with **2** for (a and b) 0.5 h and (c and d) 3 h. Scale bar = 10 μm; [dye] = 5 μM.

Some commercially available fluorescence dyes, such as CellTracker Green^{TM}, stain the entire cell; only the cytoplasm of the cells, however, was stained by the TPE dyes, presumably owing to their hydrophobic nature. Water-soluble fluorogens such as CellTracker Green^{TM} can enter the cells through the cell membrane. As they are genuinely dissolved in the aqueous medium, their isolated molecules can enter the nucleus via the nuclear pores. Therefore, these dyes can label both the cytoplasm and the nuclear compartments of the cells. In contrast, the major route for the nanoaggregates of **2** to enter a living cell is through endocytosis. During the process, the nanoaggregates are enclosed by the cell membrane to form small vesicles that can be

internalized by the cell. Inside the cell, the aggregates can be further processed in endosomes and lysosomes and are eventually released from the cellular organelles. The hydrophobic nature of the aggregates prevents them from entering the nucleus. When the nanoaggregates are bound to the biomacromolecules in the cytoplasm, they emit more intensely owing to the additional physical restriction to their intramolecular rotations.

Close inspection of the cell image reveals some highly emissive particles in the cytoplasm. These fluorescent spots may correspond to vesicles (endosomes, lysosomes, etc.) with large amounts of TPE nanoaggregates. To prove that the dye aggregates enter the cell through endocytosis, we performed the cell staining at different time intervals. The fluorescence images were taken with an inverted fluorescence microscope to have a better comparison of their brightness. Photographs were obtained in black and white and pseudocoloured green, which was the same colour emitted by **2** in the aggregate state.

The HeLa cells were first incubated with **2** for 30 min. As shown in Fig. 5b, the nanoaggregates of **2** light up the whole cytoplasm of the cell uniformly. Many dark spots are also observed. The nanoaggregates of **2** may have entered the cell membrane but not yet accumulated in the vesicles because of insufficient incubation time. As expected, the vesicles become emissive when the incubation time is prolonged to 3 h.

The nanoaggregates of **2** can selectively stain the cytoplasm of the cells, endowing them with a unique advantage over commercial CellTracker, which stains the entire cells. In most cases, it is necessary to use two different fluorogenic dyes to stain a cell: one to stain DNA in the nucleus, with the other to stain the cytoplasm surrounding the nucleus. The fluorescent dyes we developed here are therefore useful staining agents when combined with a DNA-staining fluorogen. The nanoaggregates of **2** can specifically accumulate in the vesicles of the living cells, making them promising for the tracing of the endocytosis process.

Conclusions

In this work, a series of tetraphenylethene derivatives (**1**–**4**) with varied emission colours were designed and synthesized. Whereas they are practically non-emissive in dilute solutions, they are induced to emit intensely by aggregate formation, demonstrating a novel phenomenon of AIE. Restriction of intramolecular motions is responsible for this effect. A multilayer EL device using **2** as emitter was fabricated, which emits green light with a maximum luminance and current efficiency of 12930 cd m^{-2} and 3.04 cd A^{-1} respectively. The nanoaggregates of **1**–**4** are highly emissive and cytocompatible, enabling their use for sensitive and selective imaging the cytoplasm of living cells. Further synthesis of red-emitting AIE luminogens and investigation of their biological application are under way in our laboratories.

Acknowledgement

This work was partially supported by the Research Grants Council of Hong Kong (Project numbers 603509, HKUST13/CRF/08 and HKUST2/CRF/10), the Innovation and Technology Commission (ITP/008/09NP), the University Grants Committee of Hong Kong (AoE/P-03/08) and the National Science Foundation of China (20974028). B.Z.T. acknowledges the support of the Cao Guangbiao Foundation of Zhejiang University and Dr Jiaxin Sun and Professor Hoi Sing Kwok in the Department of Electronic and Computer Engineering in Hong Kong University of Science and Technology for the electroluminescence measurement.

References

[1] (a) S. M. Borisov, O. S. Wolfbeis, *Chem. Rev.* **2008**, *108*, 423. doi:10.1021/CR068105T
(b) Y. Wang, J. Y. J. Shyy, S. Chien, *Annu. Rev. Biomed. Eng.* **2008**, *10*, 1. doi:10.1146/ANNUREV.BIOENG.010308.161731
(c) S. B. VanEngelenburg, A. E. Palmer, *Curr. Opin. Chem. Biol.* **2008**, *12*, 60. doi:10.1016/J.CBPA.2008.01.020
(d) D. W. Domaille, E. L. Que, C. J. Chang, *Nat. Chem. Biol.* **2008**, *4*, 168. doi:10.1038/NCHEMBIO.69
(e) A. Mayer, S. Neuenhofer, *Angew. Chem. Int. Ed. Engl.* **1994**, *33*, 1044. doi:10.1002/ANIE.199410441

[2] (a) B. N. G. Giepmans, S. R. Adams, M. h. Ellisman, R. Y. Tsien, *Science* **2006**, *312*, 217. doi:10.1126/SCIENCE.1124618
(b) X. Michalet, F. F. Pinaud, L. A. Bentolila, J. M. Tsay, S. Doose, J. J. Li, G. Sundaresan, A. M. Wu, S. S. Gambhir, S. Weiss, *Science* **2005**, *307*, 538. doi:10.1126/SCIENCE.1104274
(c) S. W. Thomas III, G. D. Joly, T. M. Swager, *Chem. Rev.* **2007**, *107*, 1339. doi:10.1021/CR0501339
(d) A. Burns, H. Ow, U. Wiesner, *Chem. Soc. Rev.* **2006**, *35*, 1028. doi:10.1039/B600562B
(e) N. L. Rosi, C. A. Mirkin, *Chem. Rev.* **2005**, *105*, 1547. doi:10.1021/CR030067F

[3] (a) I. L. Medintz, H. T. Uyeda, E. R. Goldman, H. Mattoussi, *Nat. Mater.* **2005**, *4*, 435. doi:10.1038/NMAT1390
(b) J. M. Klostranec, W. C. W. Chan, *Adv. Mater.* **2006**, *18*, 1953. doi:10.1002/ADMA.200500786

[4] (a) F. C. Krebs, S. R. Miller, B. J. Catalone, R. Fichorova, D. Anderson, D. Malamud, M. K. Howett, B. Wigdahl, *Antimicrob. Agents Chemother.* **2002**, *46*, 2292. doi:10.1128/AAC.46.7.2292-2298.2002
(b) H. Li, Q. Zhou, W. Liu, B. Yan, Y. Zhao, G. Jiang, *Sci. China Ser. Biol. Chem.* **2008**, *51*, 393. doi:10.1007/S11426-008-0057-9

[5] I. Chen, A. Y. Ting, *Curr. Opin. Biotechnol.* **2005**, *16*, 35. doi:10.1016/J.COPBIO.2004.12.003

[6] (a) M. Sameiro, T. Gonçalves, *Chem. Rev.* **2009**, *109*, 190. doi:10.1021/CR0783840
(b) A. Loudet, K. Burgess, *Chem. Rev.* **2007**, *107*, 4891. doi:10.1021/CR078381N

[7] (a) F. h. Quina, E. A. Lissi, *Acc. Chem. Res.* **2004**, *37*, 703. doi:10.1021/AR030152+
(b) I. Capek, *Adv. Colloid Interface Sci.* **2002**, *97*, 91. doi:10.1016/S0001-8686(01)00049-5

[8] (a) J.-L. Mergny, J.-C. Maurizot, *ChemBioChem* **2001**, *2*, 124. doi:10.1002/1439-7633(20010202)2:2<124::AID-CBIC124>3.0.CO;2-L
(b) J. L. Mergny, *Biochemistry* **1999**, *38*, 1573. doi:10.1021/BI982208R
(c) N. Venkatesan, Y. J. Seo, B. H. Kim, *Chem. Soc. Rev.* **2008**, *37*, 648. doi:10.1039/B705468H

[9] (a) J. Luo, Z. Xie, J. W. Y. Lam, L. Cheng, H. Chen, C. Qiu, H. S. Kwok, X. Zhan, Y. Liu, D. Zhu, B. Z. Tang, *Chem. Commun.* **2001**, 1740. doi:10.1039/B105159H
(b) J. Chen, C. C. W. Law, J. W. Y. Lam, Y. Dong, S. M. F. Lo, I. D. Williams, D. Zhu, B. Z. Tang, *Chem. Mater.* **2003**, *15*, 1535. doi:10.1021/CM021715Z
(c) J. Chen, B. Xu, X. Ouyang, B. Z. Tang, Y. Cao, *J. Phys. Chem. A* **2004**, *108*, 7522. doi:10.1021/JP048475Q
(d) H. Tong, Y. Dong, M. Haussler, J. W. Y. Lam, H. H. Y. Sung, I. D. Williams, J. Sun, B. Z. Tang, *Chem. Commun.* **2006**, 1133. doi:10.1039/B515798F
(e) Q. Zeng, Z. Li, Y. Dong, C. Di, A. Qin, Y. Hong, Z. Zhu, C. K. W. Jim, G. Yu, Q. Li, Z. Li, Y. Liu, J. Qin, B. Z. Tang, *Chem. Commun.* **2007**, 70. doi:10.1039/B613522F
(f) Y. Dong, J. W. Y. Lam, A. Qin, J. Sun, J. Liu, Z. Li, J. Sun, H. H. Y. Sung, I. D. Williams, H. S. Kwok, B. Z. Tang, *Chem. Commun.* **2007**, 3255. doi:10.1039/B704794K
(g) H. Tong, Y. Hong, Y. Dong, M. Haussler, J. W. Y. Lam, Z. Li, Z. Guo, Z. Guo, B. Z. Tang, *Chem. Commun.* **2006**, 3705. doi:10.1039/B608425G

[10] (a) Y. T. Wu, M. Y. Kuo, Y. T. Chang, C. C. Shin, T. C. Wu, C. C. Tai, T. H. Cheng, W. S. Liu, *Angew. Chem. Int. Ed.* **2008**, *47*, 9891. doi:10.1002/ANIE.200802560
(b) C. J. Bhongale, C. W. Chang, C. S. Lee, E. W. G. Diau, C. S. Hsu, *J. Phys. Chem. B* **2005**, *109*, 13472. doi:10.1021/JP0502297
(c) Z. Xie, B. Yang, W. Xie, L. Liu, F. Shen, H. Wang, X. Yang, Z. Wang, Y. Li, M. Hanif, G. Yang, L. Ye, Y. Ma, *J. Phys. Chem. B* **2006**, *110*, 20993. doi:10.1021/JP064069Q
(d) C. X. Yuan, X. T. Tao, L. Wang, J. X. Yang, M. h. Jiang, *J. Phys. Chem. C* **2009**, *113*, 6809. doi:10.1021/JP8111167
(e) Z. Yang, Z. Chi, T. Yu, X. Zhang, M. Chen, B. Xu, S. Liu, Y. Zhang, J. Xu, *J. Mater. Chem.* **2009**, *19*, 5541. doi:10.1039/B902802A
(f) Z. J. Ning, Z. Chen, Q. Zhang, Y. L. Yan, S. X. Qian, Y. Cao, H. Tian, *Adv. Funct. Mater.* **2007**, *17*, 3799. doi:10.1002/ADFM.200700649
(g) G. Qian, B. Dai, M. Luo, D. Yu, J. Zhan, Z. Zhang, M. Dongge, Z. Y. Wang, *Chem. Mater.* **2008**, *20*, 6208. doi:10.1021/CM801911N
(h) W. X. Tang, Y. Xiang, A. J. Tong, *J. Org. Chem.* **2009**, *74*, 2163. doi:10.1021/JO802631M
(i) J. He, B. Xu, F. Chen, H. Xia, K. Li, L. Ye, W. Tian, *J. Phys. Chem. C* **2009**, *113*, 9892. doi:10.1021/JP900205K
(j) E. Quartapelle Procopio, M. Mauro, M. Panigati, D. Donghi, P. Mercandelli, A. Sironi, G. D'Alfonso, L. De Cola, *J. Am. Chem. Soc.* **2010**, *132*, 14397. doi:10.1021/JA106772V

[11] (a) H. Tong, Y. Hong, Y. Dong, M. Haussler, Z. Li, J. W. Y. Lam, Z. Li, Y. Dong, H. H. Y. Sung, I. D. Williams, B. Z. Tang, *J. Phys. Chem. B* **2007**, *111*, 11817. doi:10.1021/JP073147M
(b) Y. Dong, J. W. Y. Lama, A. Qin, J. Liu, Z. Li, B. Z. Tang, *Appl. Phys. Lett.* **2007**, *91*, 11111. doi:10.1063/1.2753723

[12] (a) Y. Hong, M. Haeussler, J. W. Y. Lam, Z. Li, K. K. Sin, Y. Dong, H. Tong, J. Liu, A. Qin, R. Renneberg, B. Z. Tang, *Chemistry* **2008**, *14*, 6428. doi:10.1002/CHEM.200701723
(b) Y. Hong, H. Xiong, J. W. Y. Lam, M. Haessler, J. Liu, Y. Yu, Y. Zhong, H. H. Y. Sung, I. D. Williams, K. S. Wong, B. Z. Tang, *Chemistry* **2010**, *16*, 1232. doi:10.1002/CHEM.200900778
(c) Y. Hong, C. Feng, Y. Yu, J. Liu, J. W. Y. Lam, K. Q. Luo, B. Z. Tang, *Anal. Chem.* **2010**, *82*, 7035. doi:10.1021/AC1018028
(d) H. Tong, Y. N. Hong, Y. Q. Dong, M. Haussler, J. W. Y. Lam, Z. Li, Z. F. Guo, Z. H. Guo, B. Z. Tang, *Chem. Commun.* **2006**, 3705. doi:10.1039/B608425G
(e) Y. Yu, Y. Hong, C. Feng, J. Liu, J. W. Y. Lam, M. Faisal, K. M. Ng, K. Q. Luo, B. Z. Tang, *Sci. China Ser. B: Chem.* **2009**, *52*, 15. doi:10.1007/S11426-009-0008-0
(f) T. Sanji, K. Shiraishi, M. Tanaka, *ACS Appl. Mater. Interfaces* **2009**, *1*, 270. doi:10.1021/AM800224R

[13] M. Wang, G. Zhang, D. Zhang, D. Zhu, B. Z. Tang, *J. Mater. Chem.* **2010**, *20*, 1858 and references therein. doi:10.1039/B921610C

[14] Z. Zhao, S. Chen, X. Shen, F. Mahtab, Y. Yu, P. Lu, J. W. Y. Lam, H. S. Kwok, B. Z. Tang, *Chem. Commun.* **2010**, *46*, 686. doi:10.1039/B915271G

[15] Y. Q. Dong, J. W. Y. Lam, A. Qin, J. X. Sun, J. Z. Liu, Z. Li, J. Z. Sun, H. H. Y. Sung, I. D. Williams, H. S. Kwok, B. Z. Tang, *Chem. Commun.* **2007**, 3255. doi:10.1039/B704794K

[16] R. J. Ellis, *Curr. Opin. Struct. Biol.* **2001**, *11*, 500. doi:10.1016/S0959-440X(00)00239-6